Transformations in Wrinkle Patterns: Cooperation between Nanoscale Cross-Linked Surface Layers and the Submicrometer Bulk in Wafer-Spun, Plasma-Treated Polydimethylsiloxane

ARTICLE *in* NANO LETTERS · AUGUST 2009

Impact Factor: 13.59 · DOI: 10.1021/nl901136u · Source: PubMed

5 AUTHORS, INCLUDING:

H. T. Evensen
University of Wisconsin - Platteville
14 PUBLICATIONS **206** CITATIONS
SEE PROFILE

Robert W Carpick
University of Pennsylvania
222 PUBLICATIONS **6,339** CITATIONS
SEE PROFILE

NANO LETTERS

XXXX
Vol. xx, No. x
-

Transformations in Wrinkle Patterns: Cooperation between Nanoscale Cross-Linked Surface Layers and the Submicrometer Bulk in Wafer-Spun, Plasma-Treated Polydimethylsiloxane

H. T. Evensen,[†] H. Jiang,[⊥,#,‡] K. W. Gotrik,[§,¶] F. Denes,[||,#] and R. W. Carpick*[,▽]

Department of Chemistry and Engineering Physics, University of Wisconsin-Platteville, Department of Engineering Physics, Department of Biological Systems Engineering, Thin Film Deposition Center, Center for Plasma Aided Manufacturing, University of Wisconsin-Madison, and Department of Mechanical Engineering and Applied Mechanics, University of Pennsylvania

Received April 8, 2009; Revised Manuscript Received June 15, 2009

ABSTRACT

We demonstrate control of the topography of strain-induced wrinkle patterns through the interplay between the bulk and the nanoscale cross-linked top layer of plasma treated, spin-coated polydimethylsiloxane (PDMS) thin films. The different morphological phases observed, varying from herringbones to caps, are in agreement with recent theoretical predictions. The cap phase exhibits short-range 3-fold-symmetric close-packed self-organization, demonstrating a bottom-up pathway toward the wafer-scale production of ordered, nanoscale patterns on surfaces.

The morphological texturing of surfaces via wrinkling due to compressive surface strain involves the intersection of geometrical, physical, mechanical, and material phenomena. The scientific understanding of the origins and controlling factors of compression-induced wrinkling have advanced recently due to new insights derived from applying the well-known, energetically driven preference that membranes prefer to bend instead of stretch to reach a desired deflection.[1−3] The applications of these ongoing insights are significant, as surface texturing can be used to control the wettability, biocompatibility, frictional, and optical characteristics of a material;[4−7] surface texturing can also be used to determine thin film properties.[8] Compliant, wrinkled membranes also afford opportunities for novel electronic devices built on flexible substrates.[9] Controlled patterning from the nanometer to the micrometer scale is also important for technological applications such as the fabrication of micro/nanoelectronic circuits and digital storage media.[10,11] Recently, hierarchical wrinkling patterns on PDMS were applied to prevent biofouling in seawater[12] and from lithography-free microcontact printing.[13] Control of the submicrometer scale morphology is key to both applications, and creation of new morphologies will further extend the usefulness of the technique, particularly if they can be integrated with wafer-scale processing methods like the method discussed here.

Bulk samples of polydimethylsiloxane (PDMS) are known to form wavy, textured surface patterns under a variety of preparations with lateral feature sizes from ∼50 nm up to several micrometers.[8,14−18] The samples typically consist of PDMS slabs with a thin surface layer. The surface layer may consist of oxidized, silica-like PDMS produced by exposure to an oxygen[14,19,20] or argon[17,18,21] plasma, or it may consist of thin metal layers[1,2,22] or polymer or semiconductor films[7,23] deposited onto the PDMS slab.

* To whom correspondence should be addressed. E-mail: carpick@seas.upenn.edu.
[†] Department of Chemistry and Engineering Physics, University of Wisconsin-Platteville.
[§] Department of Engineering Physics, University of Wisconsin-Madison.
[||] Department of Biological Systems Engineering, University of Wisconsin-Madison.
[⊥] Thin Film Deposition Center, University of Wisconsin-Madison.
[#] Center for Plasma Aided Manufacturing, University of Wisconsin-Madison.
[▽] Department of Mechanical Engineering and Applied Mechanics, University of Pennsylvania.
[‡] Presently at: Department of Chemistry and Biochemistry, University of Texas at Arlington.
[¶] Presently at: Materials Science and Engineering department at the Massachusetts Institute of Technology.

10.1021/nl901136u CCC: $40.75

The origin of the surface feature formation is reasonably well understood. When placed under compressive strain through relaxation of the substrate, the stiffer surface layer spontaneously wrinkles to relieve the strain, producing the observed features.[24] The compressive strain can be applied either (1) anisotropically, through the relaxation of a uniaxially prestrained substrate, after forming the top layer; or (2) isotropically, due to the mismatched thermal expansion coefficients of the PDMS and the surface layer, whereby the PDMS, upon cooling, contracts far more than the surface layer. The heating may come from the plasma itself in the case of plasma-treatment methods, or from external sources. Strain may also result from the materials' differing vapor absorption properties, such that the layers swell at different rates in the presence of humidity or other chemical vapors.[25−27]

With isotropic strain, the resulting wrinkle patterns exhibit very short-range periodic order, but long-range disorder. Long-range order can be imposed by applying uniaxial strain to the material before or after treatment.[8,16,23,28] The existing body of work demonstrates the possibility of generating ordered periodic polymeric structures using straightforward, nonlithographic techniques.

A simple, two-layer mechanical model has been used to describe the coupled scaling of the wavelength and amplitude of the wrinkles. Cerda and Mahadevan[3] conducted an analysis of the wrinkling of a thin elastic sheet on a thick elastic substrate. They minimized the total energy, consisting of the bending energy of the sheet and stretching energy of the substrate, to show that the sheet's wrinkle wavelength increases with (1) the thickness of the sheet t, and (2) the ratio of the Young's moduli of the two materials, E/E_s, where E is the modulus of the sheet and E_s is the modulus of the substrate. The strength of the scaling relationships depends on the relative dimensions of the wrinkle wavelength and the thicknesses of the substrate and the sheet. The analysis also showed that the ratio of the wrinkle amplitude to the wrinkle wavelength scales with the square root of the imposed compressive strain. Previous work has elucidated several experimental scaling results. In general, it has been observed that increased plasma exposure, via either increased exposure time or power, leads to larger-scale surface features. This has been attributed to the thickening of the silica-like layer at the surface, thus increasing its stiffness and, correspondingly, the wrinkle wavelength. This effect has been seen both with plasmas[19] and with focused ion beam exposure.[29] Further, Zhao et al.[17] demonstrated that smaller wrinkling wavelengths (down to ~500 nm) could be obtained on thin, spin-coated PDMS films on silicon wafer substrates; this trend was extended to thinner films (>80 nm) and smaller wavelengths (>50 nm) by Tserepi et al.[14]

In this work, we have pursued smaller surface features by oxidizing very thin (<400 nm), spin-coated films of PDMS. Our approach is distinct from previous work in that (1) we have used thin, high viscosity liquid PDMS films, that is, with no cross-linking agent; (2) our films are spin-coated onto silicon wafers, avoiding the use of thick slabs of PDMS; and (3) we used an argon plasma instead of the common oxygen plasma. We note that preliminary results using an oxygen plasma demonstrated qualitatively similar results, except at very short exposure times as discussed below. At low film thickness, we observe a previously unreported transition from the known "wavelike" morphology to a "caplike" morphology. Additionally, we have observed a scaling with plasma treatment time that is the opposite of that reported previously; for identical film thicknesses, we observe shorter wrinkle wavelengths with increased plasma exposure time. Depth profiling by X-ray photoelectron spectroscopy (XPS) reveals the following three distinct compositional regions: an ~30 nm thick oxygen rich layer (compared with pure PDMS) with a (decreasing, increasing) amount of (oxygen, carbon) as a function of depth; a uniform ~30−40 nm thick oxygen-rich region; and then a uniform region where carbon is more prevalent (close to the composition of pure PDMS). We note that a film exposed extremely briefly (3 s) to the argon plasma did not exhibit any wrinkles immediately upon removal from the plasma chamber, but wrinkles developed slowly (within hours) with the exposure to atmosphere, which indicates that oxidization results from the ambient exposure of the films. For oxygen plasmas (3 s), no wrinkles were seen either, but a locally applied stress produced cracks in the films, indicating the presence of tensile stress in this case; this will be discussed further below.

Samples are prepared as follows. High-viscosity (100 000 cs; molecular weight = 139 000) pure liquid PDMS (Sigma Aldrich, Inc.) was dissolved in toluene at mass ratios from 20:1 to 50:1. The solutions were spin-coated directly onto single side polished 200 mm Si wafers at 6000 rpm for 60 s (Laurell Technologies Corp. WS-400B-6NPP-LITE), yielding films 80−400 nm thick. The films were all 15−20% thicker at the center of the wafer compared to the edge, as determined via ellipsometry (J. A. Woollam Co., Inc., model M-44). The reported thicknesses correspond to ellipsometry measurements taken within 5 mm of the atomic force microscope (AFM) images presented. The continuous variation of film thickness with radius was exploited to gain access to a smoothly varying range of thicknesses. All films below ~200 nm thickness were stable with no observable defects up until at least one month after their creation.

After ellipsometry measurements, the wafers were individually treated in a capacitively coupled plasma reactor. An argon plasma was employed (150 mTorr pressure, 60 sccm flow rate) with a 40 kHz source operated at 50 W. The chamber base pressure was 50 mTorr. No heating or cooling was applied to the substrate. The films were exposed for 30 or 60 s, and the chamber was vented to air and opened immediately after treatment. We did not observe any wrinkled films at the commonly used source frequency of 13.56 MHz.

Depth profiling was evaluated by XPS. The spectra were acquired using a Perkin-Elmer Physical Electronics 5400 small-area XPS system (Mg source; 15 kV; 300 W; takeoff angle 45°). Carbon, oxygen, and silicon relative atomic concentrations were evaluated using the C 1s, O 1s, and Si 2p lines.

The topographies of the wrinkled films were measured with an AFM operated in intermittent contact mode (Ambios/Quesant Instruments Q-Scope 250). A closed loop *x*-*y* scanning stage (nPoint NPXY100A) was used with the AFM for accurate metrological measurements.

The amplitude and periodicity of the wrinkle features were obtained from the AFM topographies. The periodicity was determined from the radial distribution of the two dimensional (2D) FFT of the scan image, using Image SXM (www.ImageSXM.org.co.uk) for the image processing and Mathematica (Wolfram Research, Inc.) for the fit procedure to find the predominant length scale of the features. Uncertainties were determined from the statistical output of the *NonlinearRegress* function. The amplitude was found using the histogram of the heights for each topographical scan. The heights that were greater than 10 and 90% of the scan's points were labeled as h_{10} and h_{90}, respectively, and the amplitude was defined as the difference between these, $h_{90} - h_{10}$. This height was found to match within uncertainty the height found using the more conventional approach of measuring the average peak-to-valley height difference, perpendicular to the wrinkles, at several points in the scan. The histogram technique was therefore used as a faster and more statistically rigorous method. Amplitude uncertainty was assigned as $\pm 10\%$, found by applying the *t*-distribution to the conventional peak-to-valley measurements.

Representative AFM scans of our samples are depicted in Figure 1 for a series of films with initial PDMS thicknesses t_i ranging from 116 to 332 nm. For all images, the Ar plasma exposure was 30 s. Films of 164 nm thickness or greater exhibit randomly oriented kinked or "herringbone" wrinkle patterns that are consistent with previous reports. The thickest films exhibit some loss of definition. As the thickness decreases, so too does the wrinkle's persistence length, that is, the cumulative path length along a wrinkle's "ridge" before it terminates at adjacent distinct ridges. At $t_i = 144$ nm, several isolated segments exhibit persistence lengths well below those of longer ridges. At $t_i = 129$ nm, isolated caps are seen interspersed with segments of the waves, and these caps grow in coverage at $t_i = 123$ nm. At $t_i = 116$ nm, the pattern is completely composed of caps. Thinner films (Figure 2) exhibit flat morphology. No evidence of hierarchical waves is seen in higher magnification AFM images.[16] Films treated for 60 s exhibit the same set of patterns, but with higher amplitudes for the same given thickness. The mixed phase is observed for films of thickness $130 < t_i < 165$ nm, with the pure cap phase occurring at $t_i = 114$ nm and no patterns seen at smaller thicknesses.[30]

All of these modes are exhibited in Figure 2, which shows an optical microscope image (10× magnification) of a plasma-treated 80 nm thick PDMS sample that had a streak present. This streak was apparently created during spin-casting by a contaminant on the surface and created a gradient of thickness across the streak. It is evident that its varying thickness directly affects the wrinkle morphology, proving that the pattern transition is intrinsically linked to local film thickness.

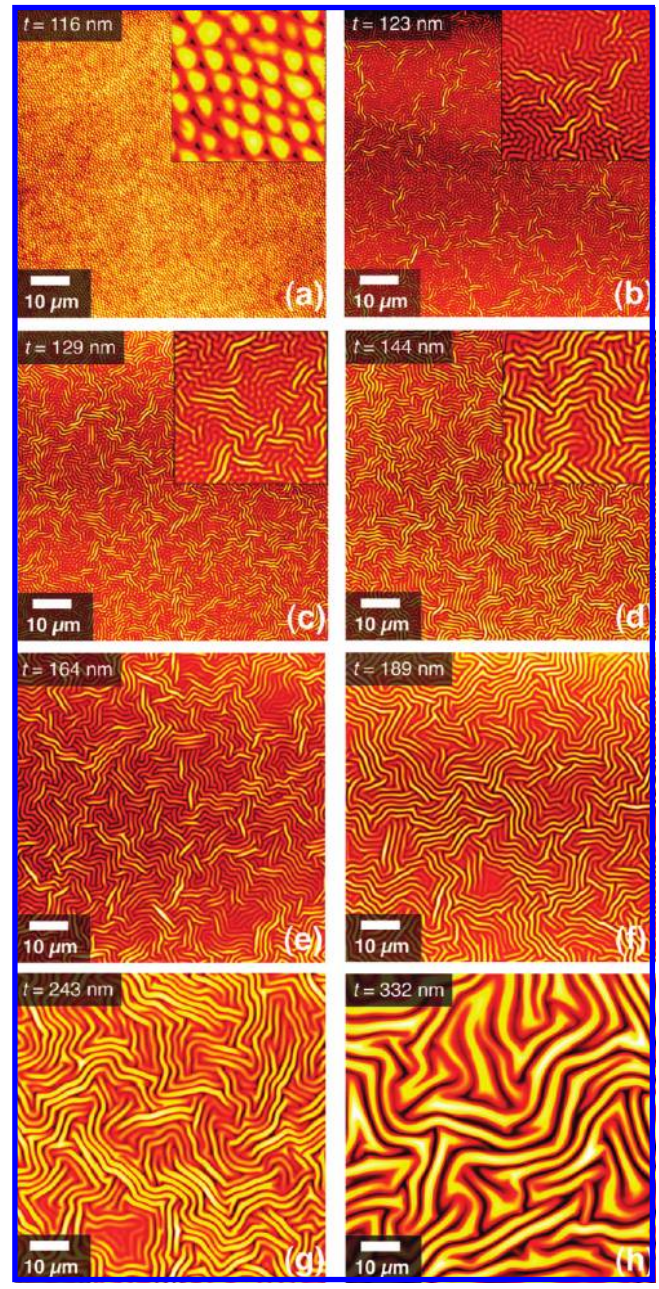

Figure 1. Representative topographical features for different thicknesses of PDMS film exposed to 30 s argon plasma. All AFM scans are 80 μm × 80 μm. The inset in (a) is 5 μm × 5 μm in size, and the insets in (b−d) are 20 × 20 μm. (a) Caplike features (film thickness = 116 nm, periodicity = 757 ± 5 nm, amplitude = 17 nm, *z*-range = 37 nm); (b) mixture of cap- and wavelike features (film thickness = 123 nm, periodicity = 781 nm, amplitude = 37 nm, *z*-range = 100 nm); (c) mixture of waves with short and long persistence (film thickness = 129 nm, periodicity = 825 nm, amplitude = 45 nm, *z*-range = 106 nm); (d) waves of increasing periodicity and persistence length (film thickness = 144 nm, periodicity = 943 nm, amplitude = 54 nm, *z*-range = 110 nm); (e) (film thicknesss = 164 nm, periodicity = 1243 nm, amplitude = 86 nm, *z*-range = 206 nm); (f) (film thickness = 189 nm, periodicity = 1415 nm, amplitude = 91 nm, *z*-range = 186 nm); (g) (film thickness = 243 nm, periodicity = 1950 nm, amplitude = 107 nm, *z*-range = 237 nm); (h) (film thickness = 332 nm, periodicity = 4130 nm, amplitude = 300 nm, *z*-range = 492 nm).

The amplitude and wavelength for both the 30 and 60 s plasma-treated films are plotted as a function of thickness

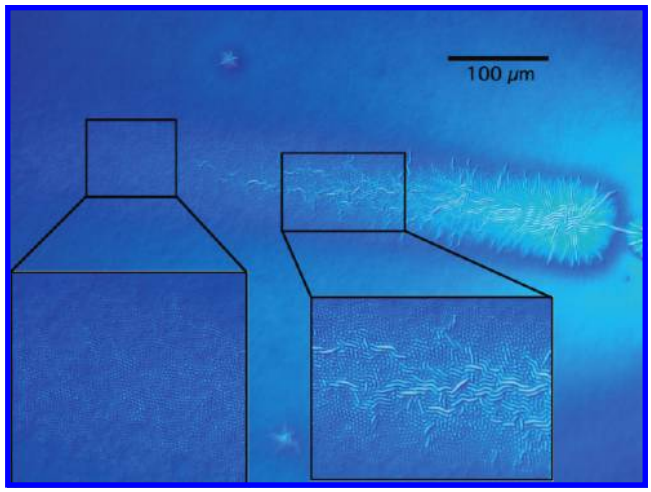

Figure 2. An optical microscope image (10× magnification) of a plasma-treated 80 nm thick PDMS sample that had a streak present. This streak was apparently created during spin-casting by a contaminant or irregularity on the surface leading to a gradient of thickness across the streak.

in Figure 3a,b respectively, with the transitions to the mixed and cap phases indicated by the different symbols. Considering the wavelength data in Figure 3b, it is seen that for $t_i >$ ~150 nm, the wavelike (longer wavelength) features can be well fit by a linear relationship, save for the very thickest films. As well, an inflection at $t_i < 150$ nm correlates with the appearance of the caplike features. Thus, the wavelength-thickness dependence changes for the caplike morphologies implying that the relationship between underlying relaxation mechanisms has changed. The wavelength appears to approach a minimum at ~500 nm.

The amplitude is plotted versus wavelength for both exposure times in Figure 4. A linear dependence is seen for wrinkles with amplitudes greater than ~50 nm, which corresponds to pure wavelike patterns with wavelengths greater than ~1 μm and thicknesses greater than ~150 nm. The 30 s plasma-exposed film has a slope of 0.067 ($R =$ 0.91) while the 60 s plasma-exposed film has a slope of 0.085 ($R = 0.98$). Further, as seen with the data in Figure 3, the slopes change with the onset of the caplike morphology, indicating a change in the dominant relaxation mechanisms.

Compositional depth profiles of the plasma-treated films were obtained by XPS; a representative scan of a ~130 nm-thick sample that features a herringbone pattern is shown in Figure 5. This data was taken several days after plasma cross-linking, when any effect of the well-known hydrophobic recovery has stabilized with time.[31] Because these depth profiling measurements require substantial acquisition times, it was not possible to obtain a complete set of scans immediately after plasma exposure, but partial scans obtained soon after initial sample preparation were consistent with these data. We see evidence of modest but rapid hydrophobic recovery via the slight increase in C concentration in the top ~2 nm. This likely means either the recovery itself is weak, or it leads to scattered nanoscale regions on the surface that are "averaged out" within the lateral resolution of XPS, consistent with previous observations.[32] We note that immediately after plasma exposure, the sample is hydrophilic, but our interest here is in the steady-state composition and structure after hydrophobic recovery.

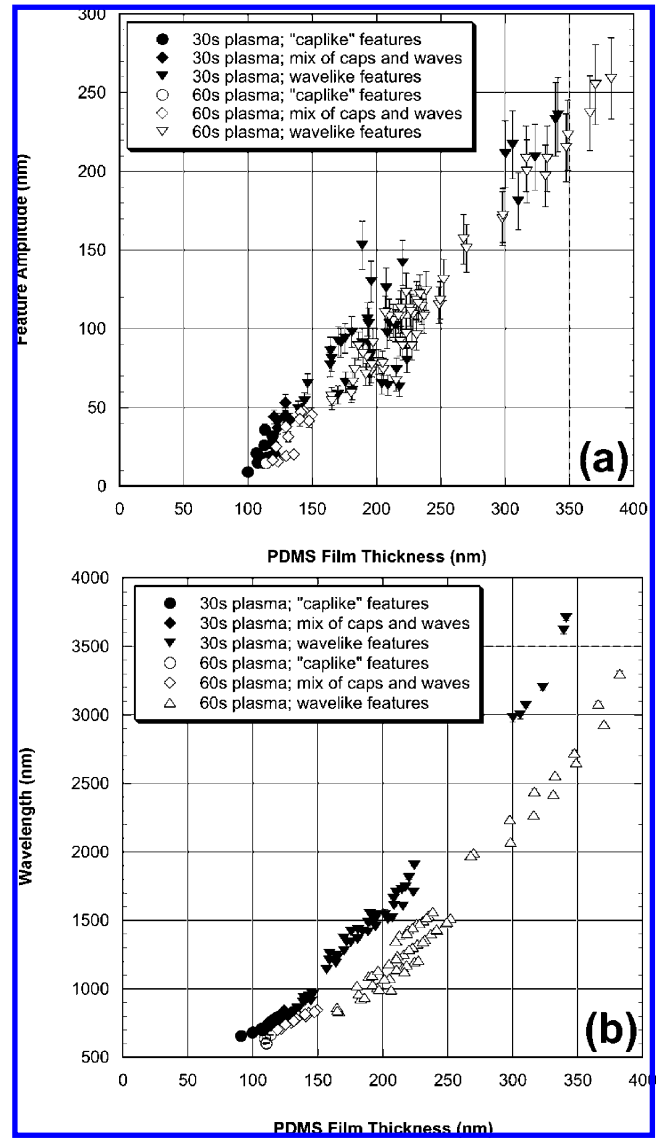

Figure 3. (a) Wrinkle amplitude vs PDMS substrate thickness for 30 s (filled symbols) and 60 s (hollow symbols) plasmas. Symbols are used to represent the different types of features: caplike (circles, ●,○), wavelike (triangles, ▼,▽), and a mixture of these (diamonds, ◆,◇). (b) Wavelength of the wrinkle features vs PDMS substrate thickness.

In this steady-state film, three layers are evident. Within approximately 30 nm of the surface, the high oxygen content is indicative of an oxidized, "silica-like" SiO_x layer,[19,20] in which methyl groups on the PDMS molecule have been replaced with oxygen atoms. Note that our XPS data shows that deeper into the material (30 to 80+ nm), the increasing carbon content occurs at the expense of decreasing oxygen content, indicating that fewer methyl groups are displaced from the polymer with increasing depth. At a depth of ~96 nm, the material more closely resembles untreated PDMS, having approximately equal silicon and oxygen concentrations with carbon being the most prevalent. Finally, deeper still, the silicon substrate is evident.

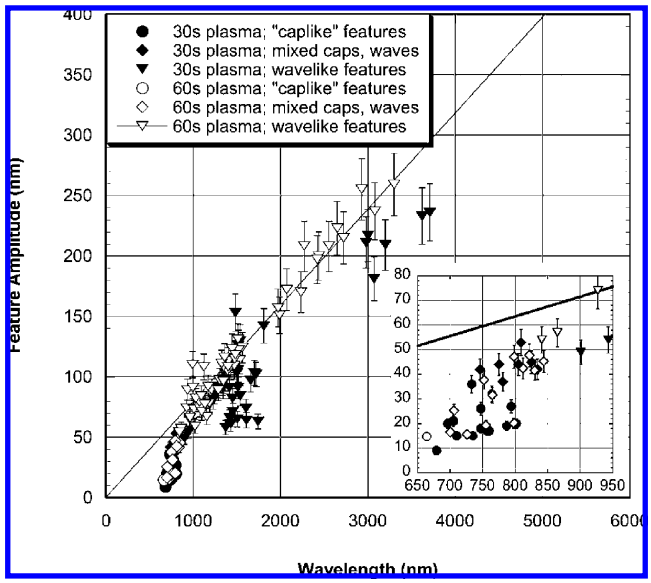

Figure 4. Wrinkle amplitude vs periodicity (wavelength) for 30 s (solid symbols) and 60 s (hollow symbols) plasmas. Symbols are used to represent the different types of features: caplike (circles, ●,○), wavelike (triangles, ▼,▽), and a mixture of these (diamonds, ◆,◇). The straight line is a least squares fit to the data for wavelike features. Inset: Zoom of the region where caplike features and the mixtures are seen.

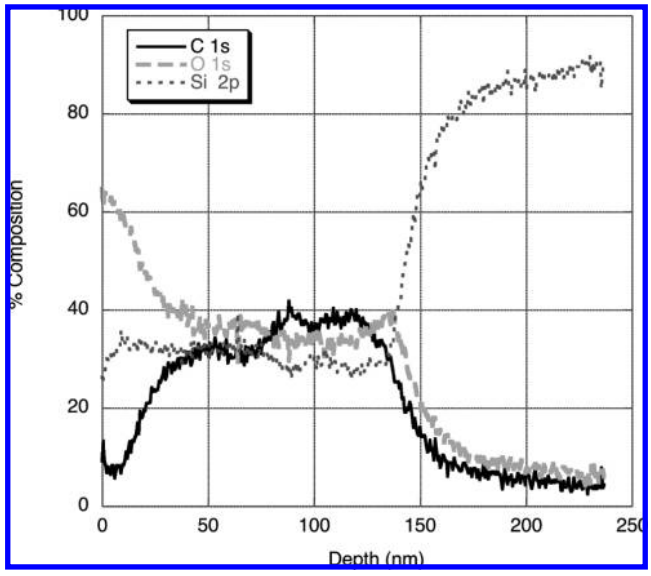

Figure 5. XPS depth profile of a spin-cast, plasma-treated film that exhibits a herringbone-like wrinkle pattern. Relative content of oxygen, silicon, and carbon are indicated.

Our observed relationship between feature periodicity and film thickness (Figure 4) for the wrinkle phase can be related to the strain energy minimization mechanism proposed by Cerda and Mahadevan,[3] which predicts that the observed wrinkling is the result of minimizing the combination of the bending energy of the stiff upper layer and the stretching energy of the elastic substrate. An equilibrium wrinkling feature is predicted in which its wavelength (λ) and amplitude (A) scale linearly with the slope related to the compressive strain[3]

$$A \sim \sqrt{\varepsilon\lambda} \quad (1)$$

The slopes of Figure 4 thus show that films treated with a 60 s plasma are under greater strain than those with the 30 s treatment. This is expected, since the longer exposure should lead to a stiffer surface layer. Furthermore, the thinner (shorter wavelength, caplike) films do not strictly follow this relationship since not only does the slope change, but the x-intercept is clearly positive. No model exists that explains or predicts this result, but we can interpret the greater slope of this region as suggestion that the surface region is under greater compressive strain for the thinner films. Note that it is not possible to calculate the strain itself from eq 1 in this case as we would need to know the Young's modulus of the top layer and the underlying film.

In fact, another source of this discrepancy may be due to the fact that Cerda and Mahadevan's model is specifically for two distinct layers (in fact, it can be used to determine the mechanical properties of nanoscale polymer films on a substrate of a different modulus[8]) However, the model is best used to provide general insight for the cases considered here, because the uppermost silica-like region is not a distinct layer in our samples, but as shown by the XPS data is in fact a region that includes a continuously varying compositional transition to the PDMS below. This is expected due both to the penetration of the plasma ions into the polymer (tens of nanometers),[33] as well as to the self-diffusion of the polymer chains throughout the substrate during treatment.[34]

In Figure 1, the feature wavelengths are five to ten times larger than the PDMS film's thickness. From Cerda and Mahadevan's model,[3] this implies the following wavelength scaling relationship:

$$\lambda \sim \sqrt{tH_s}(E/E_s)^{1/6} \quad (2)$$

Here, H_s is the thickness of the PDMS substrate, t is the thickness of the stiff outer silica-like layer, and E and E_s refer to the Young's moduli of the outer layer and the substrate, respectively. The results shown in Figure 3b are thus in qualitative agreement with this model, since the wavelength increases with film thickness. However, the dependence is much stronger than a square root relationship, especially for the 30 s treatment. This may be caused by a change in the final moduli of the materials as a function of thickness, which is discussed further below. It is noted that some variation in the thickness of the outer layer as a function of overall thickness was observed. It does not appear that this affected the observed morphologies; this will be discussed in more detail elsewhere.

Our observed progression of the surface features from "caps" to waves compares well with the results of the model developed in refs 35 and 36. These authors used nonlinear analysis of a bilayer system to simulate the two-dimensional wrinkling pattern in the film for different compressive strains. Below a critical force N_c and a corresponding critical strain, no topographic deformation was observed; at increasing

strains the pattern showed an evolution similar to that described here: from "caps" to waves. The substrate's tensile stiffness K was also found to be important; this allows the PDMS substrate to store energy, and ultimately determines the coarseness of the equilibrium wrinkle pattern.[36] If the substrate were entirely viscous, the pattern would coarsen indefinitely.

The features seen in this work can be related to the models of refs 35 and 36 by reviewing the nature of our particular system. Here, a thin, liquid polymer film was exposed to a plasma, leading to removing of methyl groups and cross-linking on the outer surface. However, a large volume of the film is affected by the plasma for several reasons. For one, previous work has shown that low-temperature plasmas can penetrate several tens of nanometers into organic films,[33] suggesting that a similar mechanism could be operating here, consistent with the data shown in Figure 5. Additionally, past studies of resist degradation under plasma exposure have shown that thermal effects of the plasma allow its mechanical effects to extend into the bulk.[37] This is because the plasma ion bombardment causes the temperature of the sample to rise, thus reducing its viscosity and increasing its self-diffusion. Therefore, self-diffusion of the polymer chains allows more material to be exposed to the plasma at the surface, and the plasma can be said to have an effect on a significant portion of the sample. The significance of the self-diffusion can be estimated using published values of the self-diffusion coefficient D for high molecular weight PDMS. From ref 38, $D \sim 5 \times 10^{-14}$ m^2/s for our material; from the definition of the diffusion coefficient $D \sim x^2/t$, one finds that a chain can diffuse across 200 nm in less than a second.

Therefore, we hypothesize that for films less than ~150−200 nm thick, the entire thickness of the film is effectively exposed to the plasma with the gradual formation of a stiff outer layer hindering this process. In fact, we observe that films of this thickness range have strong adhesion to the silicon substrate and cannot be completely removed even by submerging in piranha solution. However, all films thicker than 200 nm can be removed simply by wiping, consistent with the presence of a viscous underlayer. The plasma's effect on the liquid PDMS is thus to both create an oxidized surface layer and to cross-link the layers beneath the surface, changing a viscous liquid into an elastic cross-linked polymer. We have further evidence that the substrate layer is no longer a viscous liquid, as most of the wrinkle patterns were found to be stable and to not continue to coarsen. Conversely, the wrinkle patterns for the thickest samples, with $H_s > 250$ nm, were observed to coarsen with increasing time after leaving the plasma, suggestive of a viscous substrate.[30] For a 400 nm film, the wrinkles were observed to completely disappear after one month. Our results demonstrate the expected result that an elastic cross-linked polymer film is needed to produce sustained compressive stress on the top, oxidized layer.

With this in mind, the results shown in Figure 1 can be interpreted and better related to the results of the model in ref 35. For the thinnest films (<116 nm), no wrinkling occurs because the critical strain, which scales with the ratio of the Young's moduli of the stiffer surface film to that of the substrate, is greater than the thermally induced strain. (For films less than 150 nm thick, we hypothesize that the entire thickness of the films was oxidized, creating a stiff substrate layer.) For thicker films, the bulk material is less cross-linked, more "liquidlike," and has a lower E_s, leading to a lower N_c and a thermal strain that is now larger than the critical strain. Therefore, we see our samples generate wavelike patterns similar to those in the model with larger applied strain.

Our hypothesis for the plasma's effect on the liquid PDMS can also be used to qualitatively explain the difference between 30 and 60 s exposures shown in Figure 3b. The trend, in which longer exposure time leads to shorter wavelengths, is counter to the findings reported in most of the literature.[17,19,20] The key difference is that in our case, the plasma increases the modulus of the PDMS substrate, which from eq 2 leads to a decrease in wavelength. This effect was not seen in previous work because it was either done with a nonliquid substrate (refs 19 and 20) or with a liquid substrate for a higher plasma power and longer exposure times;[17] increased plasma exposure time thus served only to increase the thickness of the outermost layer. It should be noted that ref 18 also reported decreasing wavelength with increasing exposure time. Their work was performed on cured PDMS films (>1 μm thick) with much longer (up to 7 min) exposure times, in an oxygen plasma.

Finally, we note that other, higher-order plasma-induced reaction mechanisms could affect the wrinkle amplitude and wavelength. For one, plasma-induced etching could be affecting the wrinkle amplitude of the thinnest films. Additionally, the heat transfer from the plasma to the film, and hence the macromolecule mobility, could be affected by the film's thickness. This may influence the nature and intensity of the wrinkle formation mechanisms. Finally, plasma-induced cross-linking of PDMS also means dehydrogenation and demethylation processes that may generate shorter unsaturated bonds; resulting tensile stresses in the oxidized film from these shorter bonds could influence the wrinkle formation. This is consistent with our observation of cracks for very short exposure times in an oxygen-containing plasma.

In conclusion, we have reported plasma-induced wrinkling of thin films of high viscosity liquid PDMS and have shown transitions in the morphological features as a function of thickness, the first experimental confirmation of the predictions of recent nonlinear modeling.[35,36] Using a thick, viscous liquid polymer as the substrate allows the plasma to treat its bulk due largely to thermally enhanced self-diffusion. This leads to the plasma not only creating a stiff outer layer, but also a more elastic "substrate" layer. We are able to form submicrometer features using only spin-casting and plasma exposure, with no curing step or curing materials required. Future efforts in this area may focus on further reducing the periodicity (via stiffer substrates and/or thinner silica-like surfaces) or on achieving long-range order of the wrinkle patterns.

Acknowledgment. H.T.E. gratefully acknowledges a research grant from the University of Wisconsin-Platteville. R.W.C. gratefully acknowledges support from the Petroleum

Research Fund of the American Chemical Society, Grant #37180-G5.

References

(1) Chen, X.; Hutchinson, J. W. *J. Appl. Mech.* **2004**, *71*, 597.
(2) Chen, X.; Hutchinson, J. W. *Scr. Mater.* **2004**, *50*, 797.
(3) Cerda, E.; Mahadevan, L. *Phys. Rev. Lett.* **2003**, *90*, 074302.
(4) Oner, D.; McCarthy, T. J. *Langmuir* **2000**, *16*, 7777.
(5) Garbassi, F.; Morra, M.; Occhiello, E. *Polymer Surfaces From Physics to Technology*; Wiley: Chichester, 1994; p 462.
(6) Luk, Y. Y.; Tingey, M. L.; Hall, D. J.; Israel, B. A.; Murphy, C. J.; Bertics, P. J.; Abbott, N. L. *Langmuir* **2003**, *19*, 1671.
(7) Harrison, C.; Stafford, C. M.; Zhang, W. H.; Karim, A. *Appl. Phys. Lett.* **2004**, *85*, 4016.
(8) Stafford, C. M.; Harrison, C.; Beers, K. L.; Karim, A.; Amis, E. J.; Vanlandingham, M. R.; Kim, H. C.; Volksen, W.; Miller, R. D.; Simonyi, E. E. *Nat. Mater.* **2004**, *3*, 545.
(9) Kim, D.-H.; Ahn, J.-H.; Choi, W. M.; Kim, H.-S.; Kim, T.-H.; Song, J.; Huang, Y. Y.; Liu, Z.; Lu, C.; Rogers, J. A. *Science* **2008**, *320*, 507.
(10) Higgins, A. M.; Jones, R. A. L. *Nature* **2000**, *404*, 476.
(11) Schmid, H.; Wolf, H.; Allenspach, R.; Riel, H.; Karg, S.; Michel, B.; Delamarche, E. *Adv. Funct. Mater.* **2003**, *13*, 145.
(12) Efimenko, K.; Finlay, J.; Callow, M. E.; Callow, J. A.; Genzer, J. *ACS Appl. Mater. Interfaces* **2009**, *1* (5), 1031–1040.
(13) Pretzl, M.; Schweikart, A.; Hanske, C.; Chiche, A.; Zettl, U.; Horn, A.; Boker, A.; Fery, A. *Langmuir* **2008**, *24*, 12748.
(14) Tserepi, A.; Gogolides, E.; Tsougeni, K.; Constantoudis, V.; Valamontes, E. S. *J. Appl. Phys.* **2005**, *98*, 113502.
(15) Bowden, N.; Brittain, S.; Evans, A. G.; Hutchinson, J. W.; Whitesides, G. M. *Nature* **1998**, *393*, 146.
(16) Efimenko, K.; Rackaitis, M.; Manias, E.; Vaziri, A.; Mahadevan, L.; Genzer, J. *Nat. Mater.* **2005**, *4*, 293.
(17) Zhao, S.; Denes, F.; Manolache, S.; Carpick, R. In *Nano-scale topographic control of polymer surfaces via buckling instabilities*, Proceedings of the SEM VIII International Congress and Exposition on Experimental and Applied Mechanics, Milwaukee, WI, 2002; Milwaukee, WI, 2002; p 162.
(18) Tsougeni, K.; Tserepi, A.; Boulousis, G.; Constantoudis, V.; Gogolides, E. *Jpn. J. Appl. Phys.* **2007**, *46*, 744.
(19) Bowden, N.; Huck, W. T. S.; Paul, K. E.; Whitesides, G. M. *Appl. Phys. Lett.* **1999**, *75*, 2557.
(20) Chua, D. B. H.; Ng, H. T.; Li, S. F. Y. *Appl. Phys. Lett.* **2000**, *76*, 721.
(21) Katzenberg, F. *Macromol. Mater. Eng.* **2001**, *286*, 26.
(22) Lacour, S. P.; Wagner, S.; Huang, Z. Y.; Suo, Z. *Appl. Phys. Lett.* **2003**, *82*, 2404.
(23) Khang, D. Y.; Jiang, H. Q.; Huang, Y.; Rogers, J. A. *Science* **2006**, *311*, 208.
(24) Hobart, K. D.; Kub, F. J.; Fatemi, M.; Twigg, M. E.; Thompson, P. E.; Kuan, T. S.; Inoki, C. K. *J. Electron. Mater.* **2000**, *29*, 897.
(25) Basu, S. K.; Bergstreser, A. M.; Francis, L. F.; Scriven, L. E.; McCormick, A. V. *J. Appl. Phys.* **2005**, *98*, 063507.
(26) Chan, E. P.; Crosby, A. J. *Soft Matter* **2006**, *2*, 324.
(27) Vandeparre, H.; Damman, P. *Phys. Rev. Lett.* **2008**, *101*, 124301 (4 pp.).
(28) Jiang, X. Y.; Takayama, S.; Qian, X. P.; Ostuni, E.; Wu, H. K.; Bowden, N.; LeDuc, P.; Ingber, D. E.; Whitesides, G. M. *Langmuir* **2002**, *18*, 3273.
(29) Moon, M. W.; Lee, S. H.; Sun, J. Y.; Oh, K. H.; Vaziri, A.; Hutchinson, J. W. *Proc. Natl. Acad. Sci. U.S.A.* 2007, *104*, 1130.
(30) Chan, V. Z. H.; Thomas, E. L.; Frommer, J.; Sampson, D.; Campbell, R.; Miller, D.; Hawker, C.; Lee, V.; Miller, R. D. *Chem. Mater.* **1998**, *10*, 3895.
(31) Hillborg, H.; Ankner, J. F.; Gedde, U. W.; Smith, G. D.; Yasuda, H. K.; Wikstrom, K. *Polymer* **2000**, *41*, 6851.
(32) Hillborg, H.; Tomczak, N.; Olah, A.; Schonherr, H.; Vancso, G. J. *Langmuir* **2004**, *20*, 785.
(33) Kalachev, A. A.; Mathauer, K.; Hohne, U.; Mohwald, H.; Wegner, G. *Thin Solid Films* **1993**, *228*, 307.
(34) Joubert, O.; Hollinger, G.; Fiori, C.; Devine, R. A. B.; Paniez, P.; Pantel, R. *J. Appl. Phys.* **1991**, *69*, 6647.
(35) Huang, Z. Y.; Hong, W.; Suo, Z. *J. Mech. Phys. Solids* **2005**, *53*, 2101.
(36) Huang, Z. Y.; Hong, W.; Suo, Z. *Phys. Rev. E* **2004**, *70*, 030601.
(37) Joubert, O.; Fiori, C.; Oberlin, J. C.; Paniez, P.; Pelletier, J.; Pons, M.; Vachette, T.; Weill, A. *J. Appl. Phys.* **1991**, *69*, 1697.
(38) Appel, M.; Fleischer, G. *Macromolecules* **1993**, *26*, 5520.

NL901136U